

Aboveground Antineutrino Detectors for Reactor Monitoring and Safeguards

B. Cabrera-Palmer^a, S. Kiff^a, J. Lund, D. Reyna^a, A. Bernstein^b, N. S. Bowden^b, S. Dazeley^b, G. Keefer^b

^a*Sandia National Laboratories California, Livermore, CA, USA*

^b*Lawrence Livermore National Laboratory, Livermore, CA, USA*

Abstract

The large flux of antineutrinos that leaves a reactor carries information about two quantities of interest for safeguards: the reactor power and fissile inventory. Our SNL/LLNL collaboration has demonstrated that antineutrino based monitoring is feasible using a relatively small cubic meter scale liquid scintillator detector at tens of meters standoff from a commercial Pressurized Water Reactor (PWR). This detector was deployed in an underground gallery that lies directly under the containment dome of an operating PWR, and provides a muon-screening effect of some 20-30 mwe earth and concrete overburden. However, many PWR facilities do not have an available underground gallery to provide the screening of muon-induced backgrounds. To address this issue, we have recently developed and fielded two new detectors: a water based design and a segmented design based upon scintillation technology. In both cases, the detectors are surrounded by half meter of passive and active shielding, and the whole assembly is enclosed in a transportable 20-foot container. The container has been deployed aboveground next to Reactor Unit 3 at the San Onofre Nuclear Generating Station (SONGS) in southern California. The water detector, doped with gadolinium to **increase the detection of neutron captures**, is based on the observation of the same inverse beta-decay process used in the liquid scintillator detectors. However, by using the Cerenkov radiation signature, it has the advantage that it is insensitive to one of the major aboveground backgrounds arising from fast neutron induced proton recoils. The **segmented** second detector comprises individual segments of liquid or plastic scintillator, with screens of a lithium-doped inorganic scintillator: $^6\text{LiF}(\text{ZnS:Ag})$. The inclusion of the $^6\text{Li}(\text{ZnS:Ag})$ allows the unique identification of neutron capture events with no contamination from normal electromagnetic interactions. The final target design is a 64-cell array of 80cm long modules. We chose to first construct a smaller 4-cell prototype that allows us to better understand the improved background rejections that we may achieve through the use of event topology. We will describe the construction and deployment of each of these technologies, and present preliminary data evaluating their performance as a possible aboveground antineutrino detection system.

1 Introduction

Nuclear reactors have served as the neutrino source for many fundamental physics experiments[1]. The techniques developed by these experiments make it possible to use these very weakly interacting particles for a practical purpose. The large flux of antineutrinos that leaves a reactor carries information about two quantities of interest for safeguards: the reactor power and fissile inventory.

Antineutrino production in nuclear reactors is a direct result of the fission of Uranium and Plutonium atoms. The antineutrinos result from the beta-decay of the neutron-rich fragments. On average, each fission is followed by the production of approximately six antineutrinos. As a result, a typical nuclear power reactor will produce approximately 10^{22} antineutrinos per second. Monitoring of the antineutrino production rate can therefore provide a direct measurement of the number of atoms undergoing fission, and therefore the thermal power and operational status of the reactor. Additional information is contained in the energy spectra of the antineutrinos. Specifically, antineutrinos arising from the ^{235}U decay chain will tend to be higher in energy than those arising from the ^{239}Pu decay chain. Therefore, as the core evolves with the consumption of ^{235}U and production of ^{239}Pu , the overall energy spectrum of antineutrinos will shift to lower energies.

Detection of reactor-induced antineutrinos is usually performed through the inverse beta-decay process. In this charged current interaction, the antineutrino interacts with a quasi-free proton in a hydrogenous material. The interaction results in final-state products of a positron and a neutron ($\nu + p \rightarrow e^+ + n$), both of which can be detected through conventional means. The cross-section for this process is small ($\sim 10^{-43} \text{ cm}^2$). However, a combination of the large flux of antineutrinos from a nuclear reactor mentioned above and a moderately sized detector (a cubic meter scale detector contains $\sim 10^{28}$ target protons) can result in several thousand interactions per day at a standoff of 10-50 meters. This is more than enough to provide the desired monitoring capabilities.

Our collaboration from Sandia National Laboratories and Lawrence Livermore National Laboratory (SNL/LLNL) has demonstrated that such antineutrino based monitoring is feasible using a relatively small cubic meter scale liquid scintillator detector at tens of meters standoff from a commercial Pressurized Water Reactor (PWR). With little or no burden on the plant operator we have been able to remotely and automatically monitor the reactor operational status (on/off), power level, and fuel burnup[2-4]. The initial detector was deployed in an underground gallery that lies directly under the containment dome of an operating PWR. The gallery is 25 meters from the reactor core center, is rarely accessed by plant personnel, and provides a beneficial screening of background radiation caused by cosmic interaction in our atmosphere.

Unfortunately, many reactor facilities do not contain an equivalent underground location. We have therefore attempted to construct a complete detector system which would be capable of operating in an aboveground location and could be transported to a reactor facility with relative ease. This aboveground system was deployed and tested at the San Onofre Nuclear Generating Station (SONGS) in southern California in 2010 and early 2011.

2 Aboveground Laboratory

The previously demonstrated antineutrino detection system will not have broad applicability to commercial nuclear reactor facilities since most plants do not contain an available location (either aboveground or belowground) that could be used for this purpose. It is therefore necessary to develop an independent system that could be deployed at any facility regardless of site-specific configurations. Our choice was to begin with a 6-meter ISO container. This provided a structural facility with the internal

strength to allow large-mass shielding and detector systems to be installed. In addition, the transportation of ISO containers is relatively straightforward. To better accommodate our internal construction, we used a “high-cube” container that provided an additional 0.5m in height compared with standard container designs. While a 12-meter container would have provided more room for additional equipment, it would have created more difficulties with structural integrity and load-centering during transportation. We also felt that maintaining the smaller 6-meter footprint would allow for more flexibility in selecting possible deployment locations. We were then able to fully outfit the container with electrical wiring, climate control and a cellular modem. In this way, the entire system was fully contained, could provide remote real-time updates on data quality and required only 4 electrical supply lines from the plant.

Any aboveground system will have to account for the increase in background rates, compared to a belowground deployment. Since the antineutrino event signature involves the correlated detection of a positron and a neutron in close time-coincidence, elevated rates of environmental gammas and/or neutrons can overwhelm the ability of any detector system to select these events. Furthermore, cosmic-ray induced showers containing multiple electromagnetic and hadronic particles in coincidence can provide a source of correlated background events which can mimic the antineutrino signature. In general, gamma-ray rates depend on the surrounding amount of concrete and other radioactive materials specific to each site and not on the overburden depth and therefore will not change much between below ground and above ground deployments. On the other hand, cosmic-ray fluxes and the accompanying hadronic showers are significantly attenuated by even a few meters of overburden. Therefore, the net effect of moving our detection systems to an aboveground deployment will be to increase the overall muon flux by about a factor of six and the neutron flux by several orders of magnitude.

To moderate the impact of increased backgrounds, we constructed a hermetic neutron shield of high-density polyethylene (HDPE). The shield is at least 45cm thick on all six sides and provides for a central detector volume of 1.5m (long) x 1.0m (wide) x 1.5m (high). Furthermore, the internal volume is fully lined with 1” thick borated polyethylene (5%) and mu-metal. To allow detector modifications and maintenance, the central volume is accessible via two removable plug-doors on opposite sides. Direct measurements with neutron detectors placed both inside and outside the shield have found that this passive shield alone reduces the fast neutron rate by a factor of 4 and the thermal neutron flux by almost an order of magnitude.

Surrounding the neutron shield on five sides is a high-quality muon veto system. The purpose of the muon veto system is to identify events which are initiated by external cosmic-muons. Such muon interactions inside the HDPE shield can generate secondary showers of particles and can create correlated backgrounds that mimic the antineutrino signature. The muon veto system is comprised of 23 overlapping panels of 2” thick plastic scintillator. This thickness provides good muon/gamma separation and each panel is readout on both ends to provide uniform efficiency. There are a few small gaps in the muon veto system due to needed seismic bracing components for the neutron shield but care was taken to maximize overlapping coverage of these gaps. In-situ measurements have shown that the overall efficiency for muon identification is greater than 99%.

3 Detector Technologies

Despite the shielding improvements mentioned above, any aboveground detector will still be required to operate in an elevated background environment. To accomplish this, two detector technologies were pursued based on their differing approaches to dealing with various background components.

Water Cerenkov Detector

A water Cerenkov detector has two very positive features. First, the fact that water is inexpensive and inherently safe provides a significant advantage for real-world deployment. Second, the detection process – observation of the Cerenkov light produced by charged particles passing through the water – is insensitive to one of the larger sources of correlated background events, fast neutron recoils. In fact, in the previous underground demonstration with a liquid scintillator detector, these fast neutron events were determined to be the primary source of correlated background events. The fast neutron can fake the antineutrino signature when the neutron slows down through scattering off of a proton and then gets captured by the desired neutron detection agent. In a standard scintillator detector, the recoiling proton can be detected and appear as if it were the initial positron from an antineutrino inverse beta-decay interaction. However, in a water Cerenkov detector, the threshold for a recoiling proton to create Cerenkov light is greater than ~ 2 GeV. This high threshold effectively precludes ever detecting these events, thus eliminating fast neutrons as a source for background contamination.

However, water Cerenkov detectors have one very serious drawback: very low light output that results in very poor energy resolution. In developing this technology, this weakness was recognized and significant effort has gone into maximizing the photon collection efficiency. The walls of the detector tank were coated with a very high-reflectivity material ($> 99\%$ reflectivity) and the photocathode coverage was raised to about 10% of the total surface area. This resulted in detection of approximately 20 photoelectrons per MeV from our final detector design.

The deployed water Cerenkov detector is approximately 1m (wide) x 1.5m (long) x 1m (high) and contains about 1000 liters of purified water. To provide the desired neutron detection, the water was doped with 0.2% GdCl_3 by weight. Gadolinium provides a high neutron capture cross-section which results in a gamma cascade totaling ~ 8 MeV. These gammas are easily detectable in the water Cerenkov detector as seen in **Error! Reference source not found.** Fig. 1.

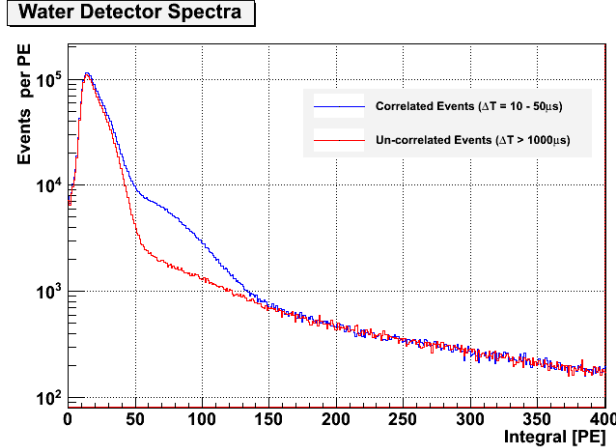


Fig. 1. Energy spectra from correlated events in the water Cerenkov detector. The blue trace shows events which are selected to have the characteristic neutron capture timing while the red trace has the opposite selection criteria. One can easily see the neutron capture events as an enhancement between 40 and 150 photoelectrons (PE).

Segmented Scintillator Detector

The development of this prototype detector was focused on enhancing background rejection through the use of unambiguous particle identification (PID) of the final-state positron and neutron. In addition, an effort was made to enhance the neutron capture and detection efficiency by avoiding the gamma-leakage associated with Gadolinium capture events in a small-scale detector. We were able to achieve both of these goals through the use of ZnS:Ag/ ^6LiF screens interleaved between standard plastic scintillator segments.

The ZnS:Ag/ ^6LiF screens are commonly used for neutron radiography. The ^6Li has a high cross-section for neutron capture (almost as high as Gadolinium) and the resulting alpha and triton do not escape the screen. In addition, these screens have relatively low sensitivity to gamma interactions. When optically coupled to a standard plastic scintillator (which has good gamma sensitivity but poor neutron detection capability), the scintillation light from the two materials can be distinguished through pulse-shape discrimination (PSD). This is relatively easy to do since the scintillation decay time-constant for the ZnS screen is $\sim 200\text{ns}$ compared with standard organic scintillators that are of order 7-10ns. One can see in Fig. 2 that the neutron capture events are very well separated from the standard gamma interactions in the plastic scintillator.

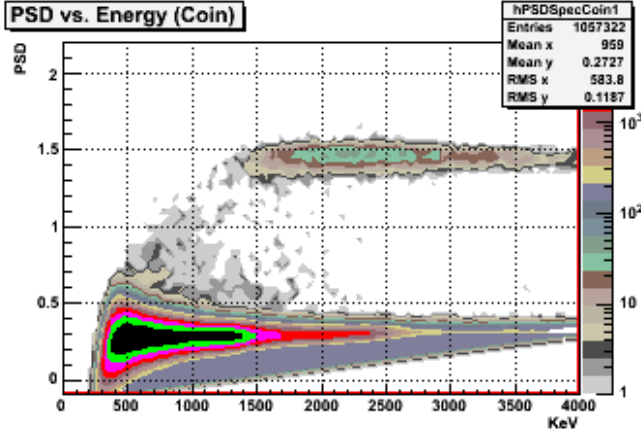


Fig. 2. Pulse Shape Discrimination as a function of Energy (KeV) of gamma and neutron-capture events with our segmented scintillation prototype detector. This data was taken with an AmBe source. The neutron capture events in the ZnS are identified with a PSD parameter greater than 1.2. They are well separated from the gamma events which interact in the plastic scintillator.

The size of the detector element was optimized to provide sufficient density of the ZnS:Ag/ ^{6}LiF screens for preferential neutron capture as well as to ensure optimal light collection for readout by PMTs at both ends. This yielded an individual segment of 13cm x 13cm x 60cm. By combining multiple elements, in a two-dimensional array, the positron final state can also be identified through a topological selection. After depositing their kinetic energy (usually in less than 1 cm), positrons produced inside the bulk plastic scintillator will annihilate producing back-to-back 511keV gammas. Those gammas will tend to travel 5-20cm. In our small 4-segment prototype, the probability that one of the neighboring segments will detect one of these gammas is \sim 30-35%. Since positrons are rare in nature, this loss in detection efficiency is expected to be more than compensated by its rejection of other background events. It is worth noting that a more stringent selection in which detection of both gammas in neighboring cells is required would have an even higher rejection of backgrounds. However, in our current 4-segment prototype, the efficiency for this selection would only be \sim 2% due to the lack of neighboring cells available.

4 Preliminary Results

The aboveground laboratory was deployed at the San Onofre Nuclear Generating Station (SONGS) in May 2010. Initially only the water Cerenkov detector was installed and it began steady data taking by the beginning of July. Preliminary analysis showed good performance of all systems. A typical inter-event time plot is shown in Fig. 3. This inter-event time distribution is used to identify events which are correlated in time and for which the second event is the result of neutron thermalization and capture on Gadolinium. The measured neutron capture time is consistent with expectations from simulation.

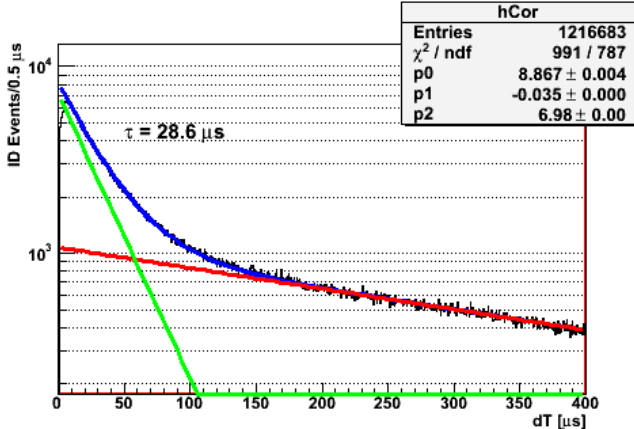


Fig. 3. Inter-event time plot for data taken by the water Cerenkov detector at SONGS. The inter-event time is the time between any two energy depositions in the detector. The shape is characterized by two expected exponentials: at long times, the exponential is governed by the random singles rate, at short times, the exponential is governed by the expected neutron capture time on Gadolinium. The neutron capture time was measured to be 28.6 μ s as shown. This is in good agreement with expectations.

While detailed analysis is ongoing, an initial effort was made to perform calibrations and gain-corrections. Then, candidate events were selected based on energy cuts and deselected based on proximity (less than 100 μ s) to external muons tagged by the muon veto. Our initial data selections found a rate of correlated pairs (candidate antineutrino events) of \sim 45,000 per day. Considering that the expected antineutrino event rate in this detector is only about 100 events per day, this represents a very significant background that would likely exclude the possibility of seeing a reactor transition.

Our initial investigations have shown that we are seeing more neutron showers than we expected. Studies of the multiplicity of neutron-capture events show that we are seeing a high-fraction (more than a third) of the events resulting from 2, 3 or more neutrons. These are particularly difficult to exclude from this event sample because the time between any two neutrons will show the same characteristic capture time as our candidate antineutrino signature. In addition, these high-multiplicity events cause multiple entries in our current pair-wise event sample. While the origin of these showers is unknown at this time, we are continuing to work on developing an algorithm for excluding the high-multiplicity events.

In December of 2010, we were able to install the 4-segment prototype scintillator detector. Due to its compact size, it was possible to operate both the water Cerenkov detector and the scintillator detector simultaneously. However, the smaller size also results in a smaller target for antineutrino interactions. With the 4-segment prototype, we calculated that the theoretical maximum interaction rate would be \sim 200 events per day with a more likely detection rate of less than 40 events per day.

We are still in the process of fully gain-correcting the data, but we can already see the results of using PID information for background rejection. If we use the same inter-event time analysis applied to the water Cerenkov detector, we find that the 4-segment scintillator detector has a background rate of over 225,000 events per day. However, by using the neutron PID information (i.e. selecting pairs of events for which the first event is clearly not a neutron and the second event clearly is a neutron), we reduce the candidate sample down to only 1,830 events per day. The results of this impressive 2 order of magnitude rejection in background can be seen in Fig. 4. This data sample is

based on only 1 week of data, but one can clearly see the characteristic exponential rise at shorter times due to the neutron capture cross-section of the ${}^6\text{Li}$.

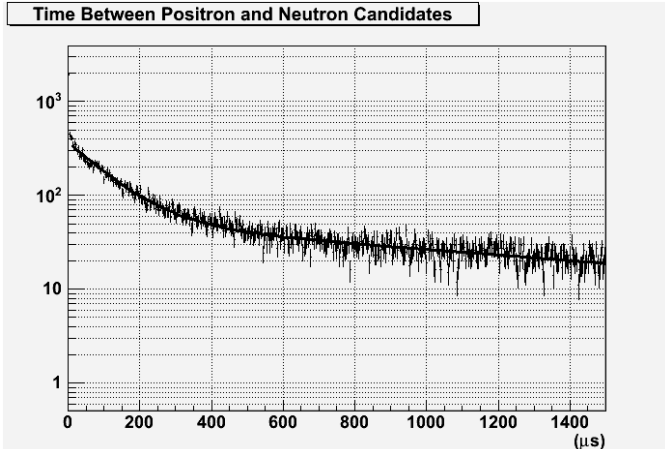


Fig. 4. Inter-event time plot taken by the 4-segment scintillation detector at SONGS. These events were selected using only the positive and negative selection of neutron PID to identify positron and neutron candidates. The resulting distribution of time between the positron and neutron candidates shows the expected neutron-capture time constant for coincident events.

As mentioned previously, further background rejections are possible by using the topological information of the individual segments to provide positron PID. Requesting one and only one neighboring segment to have less than 550keV of energy results in a background rate of 300 events per day while using the most restrictive positron definition (requiring two neighboring segments to each have less than 550keV) results in only 23 events per day. These rates are still preliminary and the detector systems need to be fully calibrated before any large conclusions can be drawn. In addition, this technology also provides good positron energy resolution, a feature which has yet to be fully exploited. Since the energy spectrum of the positrons should closely resemble the energy spectrum of the antineutrinos produced in the reactor, this can be used to provide further confidence in any claim of antineutrino detection.

5 Conclusions

The background rejections of up to 4 orders of magnitude from the segmented scintillator detector are impressive, but it remains to be seen what the efficiency for antineutrino signal acceptance may be. To do this, we need to operate our detectors during periods when the reactor is operating at full power (and thus creating antineutrinos) and during periods when the reactor is off. Then comparisons of the data from both periods can be used to look for differences in count rates that would indicate an antineutrino signature. We were fortunate that our deployment coincided with a reactor refueling and refurbishment outage lasting from October 2010 through February 2011. Both of our detector systems have now recorded at least a month of data in both reactor on and reactor off conditions.

While the water Cerenkov detector has not shown immediate promise, we still hold out hope that we may yet be able to handle the multi-neutron backgrounds in such a way that a positive reactor transition signal can be achieved. The segmented scintillator detector appears to show greater promise, but the demonstration remains to be proven. Our

deployment at SONGS will be completed at the end of June 2011 and we hope to have final results from these systems shortly thereafter.

It is worth noting that aboveground detection of antineutrinos from reactors has never before been successfully accomplished. The background rates are very high and the antineutrino signatures are very weak. However, we feel that we have made significant progress, both in the form of creating a viable transportable aboveground laboratory and in creating technologies which have the best chance of success in this environment. Having previously demonstrated that antineutrinos provide a unique method for verifying reactor operator declarations of power history and fuel content, the successful demonstration of a transportable aboveground antineutrino system could finally provide a technological path forward for the adoption of this technique into current reactor safeguards.

Acknowledgements

Sandia National Laboratories is a multi-program laboratory managed and operated by Sandia Corporation, a wholly owned subsidiary of Lockheed Martin Corporation, for the U.S. Department of Energy's National Nuclear Security Administration under contract DE-AC04-94AL85000.

References

- [1] C.L. Cowan, Jr., F. Reines, F.B. Harrison, H.W. Kruse and A.D. McGuire, "Detection of free neutrino: a confirmation," *Science*, col. 124, pp. 103-104, Jul 1956.
- [2] N.S. Bowden, *et al.*, "Experimental results from an antineutrino detector for cooperative monitoring of nuclear reactors," *Nucl. Instr. and Meth. A.*, vol 572, pp. 985-998, Mar. 2007.
- [3] A. Bernstein, N.S. Bowden, A. Misner, and T. Palmer, "Monitoring the thermal power of a nuclear reactor with a prototype cubic meter antineutrino detector," *J. Appl. Phys.*, vol. 103, no. 074905, Apr. 2008.
- [4] N.S. Bowden, *et al.*, "Observation of the isotopic evolution of pressurized water reactor fuel using an antineutrino detector," *J. Appl. Phys.*, vol. 105, no. 064902, Mar. 2009.